Natural Hazards
https://doi.org/10.1007/s11069-022-05394-9

ORIGINAL PAPER

A refined model of a typhoon near-surface wind field based on CFD

Youtian Yang[1] · Lin Dong[1] · Jiazi Li[1] · Wenli Li[1] · Dan Sheng[1] · Hua Zhang[2,3]

Received: 23 October 2021 / Accepted: 5 May 2022
© The Author(s), under exclusive licence to Springer Nature B.V. 2022

Abstract
The simulation of near-surface typhoon wind fields is crucial for high-precision typhoon hazard assessments and thus of great significance for disaster forecasting, loss risk assessment and emergency management. The terrain correction method for simulating regional large-scale wind fields has a single correction method that cannot satisfy the requirements of refined risk assessment. This paper aims to use the advantage with regard to accuracy of the fluid dynamics mechanism model (CFD, computational fluid dynamics) in small-scale wind speed simulations and obtain a terrain correction method suitable for simulating regional large-scale wind fields by extracting the spatial variation of the wind speed over complex terrain. Specifically, typical mountains with different cross-sectional shapes and slopes are used to characterize the undulating terrain, and the CFD model is used to simulate and analyze the wind speed changes on the upwind and leeward slopes, at the mountain top, and in the downwind area under different initial wind speeds. The wind speed at these locations has a good quantitative relationship with the initial wind speed. Combined with the typical building wind load codes in China, the wind speed correction algorithm suitable for large-scale complex terrain is supplemented and improved. This paper presents the simulation results of three typhoons, and taking Typhoon No. 0713 as an example, a near-surface typhoon wind field simulation is performed. Compared with that of other models, the accuracy of the terrain-corrected simulation results by the method provided in this article is increased by 8.8–16.89%. Such CFD-based typhoon disaster near-surface wind fields can more accurately reflect the spatial distribution and intensity of typhoon wind hazards over large-scale complex terrain and can provide technical support for the loss risk prediction and assessment of forest resources, mountain forestry economies, crops and other vulnerable bodies during typhoon disasters.

Keywords CFD · Near-surface wind field · Wind speed terrain correction · Typhoon disaster

✉ Hua Zhang
zhanghua2011@bnu.edu.cn

Extended author information available on the last page of the article

Published online: 22 June 2022

1 Introduction

Typhoon wind fields can reflect the differences in the spatial range and intensity of typhoon hazard factors (Weihua and Wei 2013). Therefore, the simulation of typhoon wind fields is an important prerequisite for performing typhoon disaster numerical forecasting and loss risk estimation (Qian et al. 2005). Currently, hazard assessments of Chinese typhoon hazards are often based on the CMA tropical cyclone best path dataset provided by the China Meteorological Administration that uses the central pressure and maximum wind speed data to simulate wind fields mainly for larger-scale typhoon hazards analysis or to study the evolution of typhoon paths (Jinping et al. 2002). Since the Earth's surface is host to numerous people and socioeconomic bodies that often suffer losses due to typhoon disasters, research on the high-precision simulation of near-surface typhoon wind fields is of great significance.

The temporal and spatial distribution characteristics of hazard factors are affected by regional differences in the disaster environment. The distribution of one hazard factor in particular, namely, wind during a typhoon disaster, is greatly affected by the terrain, surface roughness and other surface conditions (Alexander 2000). When air flows through hillsides, valleys and other terrains, wind speed will significantly increase or decrease (Ngo and Letchford 2009). Currently, most engineering wind load calculations adopt the topographic factor correction method in the wind load codes of various countries (Maharani 2009). To ensure the safety of engineering buildings, the wind load codes of various countries mainly focus on the acceleration effect of the terrain on the wind field; this may also be due to the safety of project site selection, so wind load codes are mostly applicable to areas with slopes gentler than 16° (Building Structure Load Code [S]. GB50009-2012). The terrain correction of wind speed based on wind load specifications ignores the deceleration effect of the leeward slope and reduces the uplift acceleration effect of the steep terrain. This assumption will lead to a significant underestimation or overestimation of risks in disaster risk analyses.

To simulate wind field over complex terrain, the application of a fluid dynamics mechanism model (CFD, computational fluid dynamics) can accurately reflect the airflow characteristics (Uchida 2018) and the flexibility and low cost of numerical simulations make this method the main approach for the study of the law of wind speed changes. Shun et al. (2009) studied the influence of terrain slope, ground roughness and atmospheric boundary layer on the wind speed of circular steep slope terrain and confirmed the feasibility of CFD for wind farm terrain turbulence. Griffiths et al. (2010) used atmospheric models and CFD to simulate mountain airflows under different slope terrains and verified that the simulation results of the two models were closer for higher slope value. However, due to the complex design of CFD and its high computational cost, it is mainly used for microscale airflow field simulations (Cheng et al. 2005). Researchers have investigated the applicability of wind load codes in various countries. Ishihara et al. (1999) studied the wind speed distribution of the three-dimensional terrain at the top, side and foot of the mountain and found that the wind speed near the foot of the windward slope decreased, but the wind speed at the top and side of the mountain significantly increased, and the wind speed at the top increased by 50–60%. Li (2010) reviewed the impact of the typical terrain on near-ground wind fields, conducted an in-depth comparison and analysis of the current wind load codes in various countries and found that identical formulation was used in the codes in various countries, but the models that described the impact of the terrain on the wind fields were different. Shen (2016) used the CFD simulation method to study the wind field of single

and double hills and found that the acceleration effect at half-hill height above the top of the mountain was weakened, and the acceleration effect of the cross-direction wind was greater than that of the wind direction. In summary, previous studies have confirmed the feasibility of CFD for studying wind fields, and some refinements and extensions of wind speed and terrain correction have been proposed. However, due to the large spatial scale affected by typhoon disasters, the direct application of CFD is difficult, so that a complete typhoon wind field model combined with CFD has not been formulated.

In summary, the direct use of CFD to simulate large-scale typhoon wind fields incurs high computational cost and is time-consuming, while the accuracy of wind speed simulations with reference to building wind load specifications is insufficient. Based on the CFD simulation of a small-scale complex terrain wind speed field, this paper extracts the wind speed characteristic curve under typical terrain conditions and combines the wind load specification to improve the large-scale complex terrain influencing factor algorithm, improving the simulation accuracy of the near-surface typhoon wind field and providing technical support for typhoon disaster risk numerical evaluation.

2 Materials and methods

2.1 Data sources

2.1.1 Typhoon path data

The historical typhoon sample data are taken from the CMA tropical cyclone best path dataset (https://tcdata.typhoon.org.cn/zjljsjj_sm.html) released by the China Meteorological Administration. This dataset includes all tropical cyclone information generated in the Northwest Pacific since 1949 (Ying et al. 2014; Lu et al. 2021).

2.1.2 Measured wind speed data at weather stations

The measured wind speed data of meteorological stations are taken from the daily value datasets of basic meteorological elements of China's national ground meteorological stations.

2.1.3 Basic data

Including DEM data [Aster (https://lpdaac.usgs.gov/products/astgtmv003/)), land use data (Base on POI (Dong 2021)].

2.2 Research methods

This paper uses CFD to simulate the wind speed of different mountains and extracts the rules governing the wind speed changes as the typhoon disaster terrain influences factor algorithm. Based on the CMA typhoon path information, the Holland parametric wind field model with the provisions of the Building Structure Load Code GB50009-2012 is used to simulate the near-surface wind field of the typhoon disaster and is verified using the measured data obtained from weather stations (Fig. 1).

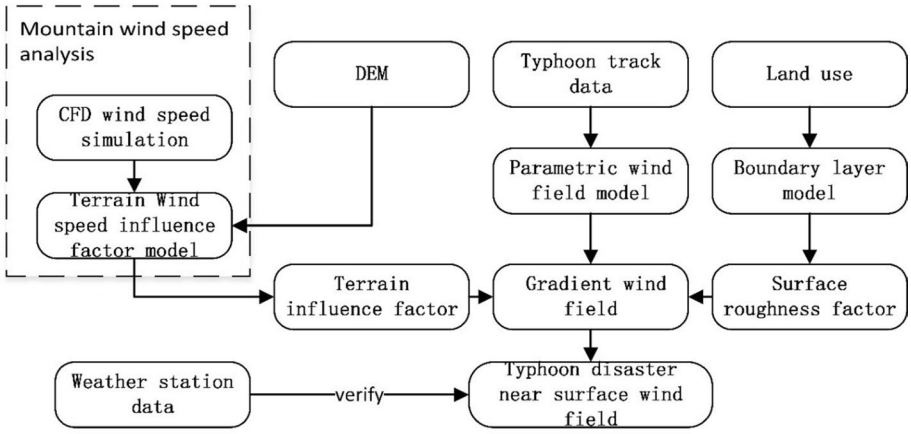

Fig. 1 Methodological procedures of the research

2.2.1 CFD technique and set-up

This article uses Rhino and its included plug-ins, such as Grasshopper and Butterfly, for CFD wind speed simulations. Rhino is used to build 3D mountain models and visualized displays. Grasshopper provides a visual programming platform and uses "battery" as the basic computing unit (https://www.grasshopper3d.com/page/tutorials-1). Butterfly is the core component of CFD solution; its kernel is based on OpenFOAM and supports Python scripts and interaction with CFD open-source software such as Blue-CFD and ParaView (https://ladybug-tools.gitbook.io/butterfly primer/). In the preprocessing stage of the CFD solution, Butterfly provides functions such as wind tunnel setting and grid division. Butterfly provides two different environment simulation solvers, namely Heat Transfer Recipe and Steady Incompressible Recipe, for temperature and wind. Three turbulence models, including the laminar turbulence model (using no turbulence models), LES turbulence model (using large-eddy simulation modeling) and RAS turbulence model (using Reynolds-averaged simulation modeling), were used. In the postprocessing stage, correlation processing of vector data is provided. Other related plug-ins include Honeybee that provides the function of setting test points in wind speed simulation and Ladybug that provides visualization functions such as grid coloring and airflow line drawing.

To explore the general laws of the changes in different mountain customs, this article sets different slope variation ranges ($\tan\alpha = 0.17$–1, i.e., angles 10, 20, 30, 45) and different cross-sectional shapes (parabolic, Gaussian, cosine) (Li et al. 2016). In total, there are 12 mountain models for CFD numerical simulation, and the simulation space is divided into a hexahedral grid that fits the surface of the mountain. Then, the test surface was set in the same direction as the initial wind speed at 10 m above the mountain and the test points were evenly distributed on the test surface. Using different initial wind speeds (15 m/s, 30 m/s) as the input, the wind speed at the test point is calculated by the RAS turbulence model and steady incompressible recipe to explore the general law of wind speed changes with the terrain undulations of the mountain. Furthermore, the test points are partitioned, and the wind speeds at the foot of the windward slope, the top of the mountain, and the foot of the leeward slope are counted. It is stipulated that $V_h = \eta \times V_0$, where V_h is the near-surface wind speed affected by the terrain, V_0 is

the near-surface free wind speed not affected by the terrain, and η is the terrain influence factor that represents the degree of change in the wind speed due to terrain undulations.

2.2.2 Gradient wind field model

For typhoon disasters, it is generally believed that when the height above the ground is 300–550 m, the wind speed is no longer affected by the surface roughness and topography; i.e., the so-called gradient wind speed is reached (Building Structure Load Code). In this paper, a mature and easy-to-calculate Holland parameterized circularly symmetrical wind field is selected to simulate the gradient wind speed (Holland 1980), and the wind field equation is:

$$V_g = \sqrt{(p_n - p_c)\frac{B}{\rho_a}\left(\frac{\mathrm{RMW}}{r}\right)^B \exp\left(-\frac{\mathrm{RMW}}{r}\right)^B + \left(\frac{rf}{2}\right)^2} - \frac{rf}{2} \tag{1}$$

$$\mathrm{RMW} = -18.04 \ln \Delta p + 110.22 \tag{2}$$

$$B = 1.38 - 0.00184\Delta p + 0.00309\mathrm{RMW} \tag{3}$$

In Formula (1), V_g is the gradient wind speed at a certain point in the typhoon range, p_n is the air pressure at the periphery not affected by the typhoon, p_c is the central air pressure of the typhoon, RMW is the maximum wind speed radius, ρ_a is the air density, f is the Coriolis parameter, r is the distance between the calculated point and the typhoon center, and B is the shape parameter of the typhoon. The estimation of the RMW parameters refers to the empirical formula of Lin et al. (2013) based on JTWC data fitting, and B is calculated using the method proposed by Vickery et al. (Vickery and Dhiraj 2008). These two calculation methods are highly applicable in the Northwest Pacific.

2.2.3 Boundary layer model

In the near-surface disasters caused by strong winds, ground friction cannot be ignored, and different surface roughness values will further affect the spatial distribution of wind speed. When the pressure field does not change with height, the wind speed mainly depends on the ground roughness and vertical temperature gradient, and the variation in the wind speed at different heights generally conforms to the exponential law given in Formula 4. Here, a is the ground roughness index corresponding to the four types of land use (sea, rural, urban and metropolitan centers), v_z is the gradient wind speed at different heights corresponding to different land use types, and v_{10} is the wind speed at a height of 10 m:

$$v_z = v_{10}\left(\frac{z}{10}\right)^a \tag{4}$$

In summary, using the terrain correction factor calculation model based on the CFD simulation results, a high-altitude gradient layer wind field model and a boundary layer model, a refined typhoon near-surface wind field model was constructed.

3 Results and analysis

3.1 CFD simulation results and terrain factor calculation

3.1.1 Analysis of the change in mountain wind speed based on CFD

In the CFD to simulations of the wind speed, since typhoon wind fields usually represent the wind speeds 10 m above the ground, the gradient wind speed reference high speed is set to 10 m; considering the surface coverage characteristics consisting of multiple-vegetation types across the mountains of southern China, the surface roughness parameter is set to 0.15 (Lou et al. 2016). Figure 2 shows the wind speed changes of the three cross-sectional mountains under different slope scenarios when 15 m/s and 30 m/s are used as the free wind speed inputs:

At the peak and foot of the mountain, the results show that under the two input wind speed conditions, the wind speed changes significantly with the variation in the height of the mountain. The wind speed increases significantly when the wind approaches the apex

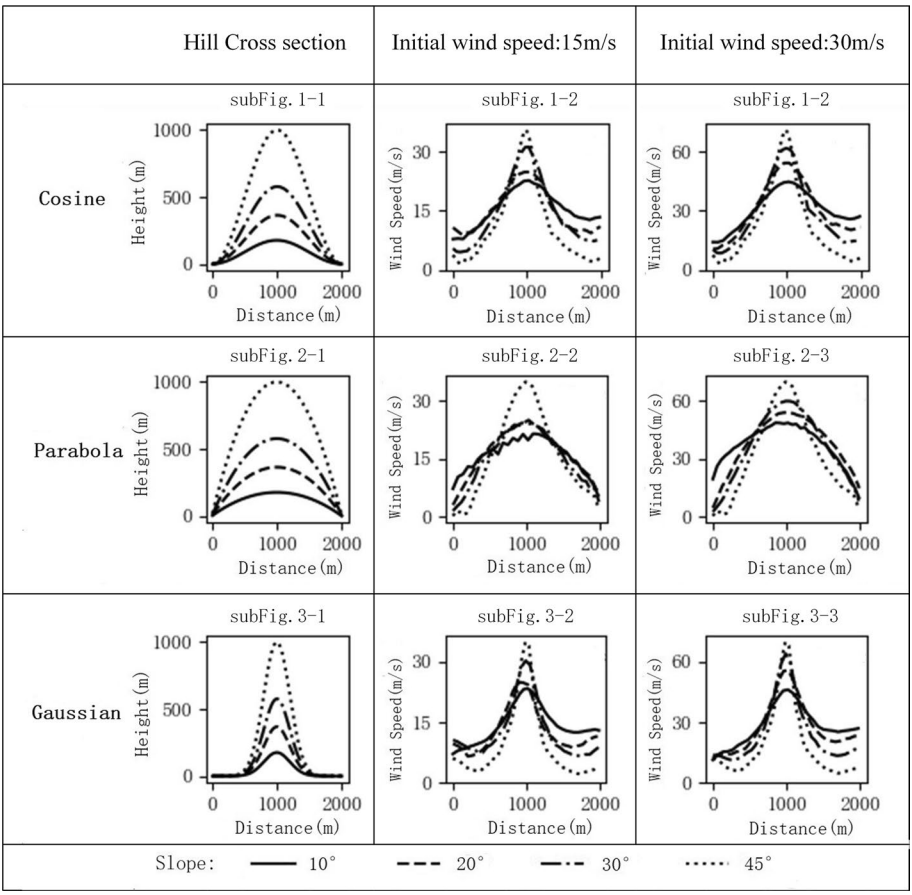

Fig. 2 CFD mountain wind speed simulation results

of the three types of mountains; when the total length of the mountain is identical, a greater a slope of the mountain (a larger height) corresponds to a more pronounced increase in the wind speed at the apex. At the foot of the windward slope and leeward slope, the wind speed decreases, and the magnitude of the decrease is related to the slope. A greater slope corresponds to a more pronounced decrease. When the slope of the mountain exceeds 16° ($\tan\alpha > 0.3$), the trend of the wind speed change with the mountain does not change, which is similar to the law of the overall wind speed of a mountain with a lower slope.

On the hillside, the wind speed distribution on the windward and leeward slopes is closer to the top of the mountain and exhibits a symmetrical shape. Outside of its range, the two wind speed distributions are different: The wind speed shows an overall increasing trend from the foot of the windward slope to the top of the mountain, and only for the Gaussian mountain, first decreases and subsequently increases when the slope is large. The wind speed at the foot of the leeward slope tends to rise; i.e., the wind speed on the leeward slope first decreases and subsequently increases. However, in most cases, the magnitude of the change is small, and the change is more pronounced only when the slope exceeds 30°.

Overall, the distribution of wind speed is very similar to the shape of the mountain itself; i.e., the terrain correction factor is not simply a continuous linear change with the distance of the mountain peak but rather varies with the shape of the mountain.

3.1.2 CFD-based terrain factor

Based on 24 sets of wind speed simulation results performed by CFD, quantitative analysis was performed, and statistical wind speed change characteristics were extracted. For the foot of the windward slope and the foot of the leeward slope, we selected the minimum wind speeds that occurred in these two areas, calculated the ratio of the input wind speed, i.e., the terrain correction coefficient (η), and combined η with the slope, mountain height and other variables. Fitting was performed, and the calculation formula of the terrain correction coefficient was obtained. For mountain apexes, the existing correction method can reflect the characteristics of the wind speed changes within its scope of application. Based on the characteristics, setting the slope correction coefficient provides a more detailed correction plan for mountains with slopes greater than 17° ($\tan\alpha > 0.3$). Since the difference in the wind speed is affected by different mountain shapes, the calculation method of η on the slope is changed to vertical interpolation to highlight the difference in the influence of different mountain shapes on the wind speed and make it closer to the real wind speed distribution. Due to the shielding effect of the mountain, the wind speed in the flat area behind the leeward slope of the mountain maintains a decreasing trend for a certain distance. The details for the calculation method are shown in Table 1:

In addition to the mountain terrain in Table 1, for other undulating terrain types such as canyons and basins, refer to the recommended values in the "Building Structure Load Code."

3.2 Simulation of a near-surface typhoon wind field

3.2.1 Typhoon wind field simulation results

This paper selects Typhoon No. 0713 (International Number 0712), Typhoon No. 1211 and Typhoon No. 1814 to simulate the wind speed by using the CFD typhoon wind field model and uses the measured wind speed data obtained at meteorological stations to verify

Table 1 Redefinition of the η calculation method based on CFD

Terrain	Specific location	Calculation method
Mountain	Windward slope	At the foot of the windward slope, the value of η is $0.62 - 0.7 \times \tan\alpha + 0.54\left(\frac{h}{H}\right)$, where h is the elevation value of the foot of the windward slope, and H is the total height of the mountain. The windward slope is vertically interpolated with the upper and lower limits of η at the top and foot of the windward slope. The interpolation model is $\eta_c = \eta_f + \frac{|h|}{H}\left(\eta_t - \eta_f\right)$
	Mountain top	$\eta = 1 + k \times m \times \tan\alpha\left(1 - \frac{z}{2.5H}\right)$, given different conversion values m for different slope intervals. Within a slope range of 17°–45° m is temporarily set to 1.2
	Leeward slope	At the foot of the leeward slope, the value of η is $0.62–0.7 \times \tan\alpha + 0.54$ (h/H). Vertical interpolation is still used on the slope. It is necessary to point out that the wind speed at the foot of the leeward slope shows a small rise that is ignored for simplified calculations on a large scale
Affected area	Downwind area	From the foot of the leeward slope to the downwind area approximately 15 times the height of the mountain (Cheng et al. 2015), the correction coefficient gradually rises to 1, which means that this area is out of the range of the terrain

the accuracy of the wind speed simulation results. Among the three typhoons, Typhoons Nos. 1211 and 0713 were similar in intensity but moved in different directions and had different shapes after landing; Typhoons Nos. 1814 and 0713 moved in similar directions but with different intensity levels and different paths during the extinction period. Therefore, these three typhoons were selected to verify the applicability of the CFD typhoon wind field model for different types of typhoons. Since the pressure near the periphery of the typhoon is not significantly different from the pressure undisturbed by the low-pressure center, the wind generated by the typhoon is not necessarily dominant in the local wind speed, so that the seven-level wind circle range is usually given as the typhoon warning range in the weather forecast. Additionally, winds below magnitude 7 rarely cause disasters, so the coastal area of China within the radius of the typhoon wind circle of magnitude 7 is selected as the verification area. The simulation results of the three typhoon cases are shown in Fig. 3.

Typhoon No. 0713 reached high wind speeds near the typhoon landing points in Cangnan County and Pingyang County in southern Zhejiang Province. This area is close to the typhoon landing center, the terrain is undulating, and the towns are sparse, further increasing the near-surface wind speed of the typhoon. Typhoon No. 1211 had a relatively strong wind speed in Xiangshan County, eastern Zhejiang Province, and the wind speed remained near the peak for a long time and moved westward into the inland area. For Typhoon No. 1814, although the intensity was low when it made landfall, it lasted for a long time. After entering Shandong Province, it still had a greater impact and eventually penetrated Northeast China. The average simulation error of the three typhoons was 19.1%. Among these, the absolute wind speed difference of No. 0713 was the highest, and that of No. 1811 was the lowest; the main reason for this difference is the influence of the intensity of the typhoon itself.

3.2.2 Verification of the typhoon wind field simulation results

For an in-depth analysis of the simulation effect and possible deficiencies of the wind field model of CFD, Typhoon No. 0713 was taken as an example. Within the 7-level wind circle of Typhoon No. 0713, the maximum absolute difference between the typhoon wind field model simulation results based on CFD and the meteorological station records is 17.8 m/s, the minimum absolute difference is 0.01 m/s, and the average error rate is 17.2%. The spatial comparison between the simulation results and the weather station records is shown in Fig. 4.

The distributions and variation trends of the meteorological station data and simulated wind speed data are similar. The wind speed is high near the landing point and then decreases as the typhoon moves inland under the influence of surface friction and its own strength attenuation and increases again in the coastal areas that leave the land and re-enter the ocean. The wind speed is a hazard factor that is highly sensitive to the terrain. From Detail 1 in Fig. 4, the horizontal distance between Point 1 at the top of the mountain and Point 2 at the foot of the mountain is only 15 km, which is quite small compared with the typhoon's influence range, but the difference in the wind speed between them is 20.3 m/s due to the influence of terrain. Restricted by the location factor of weather station site selection, most of the stations are located in areas with relatively flat terrain and rarely appear in undulating positions, such as mountain tops and hillsides, as shown in detail 2 in Fig. 4. Therefore, the spatial interpolation of meteorological station data is unlikely to accurately reflect the wind speed distribution on the

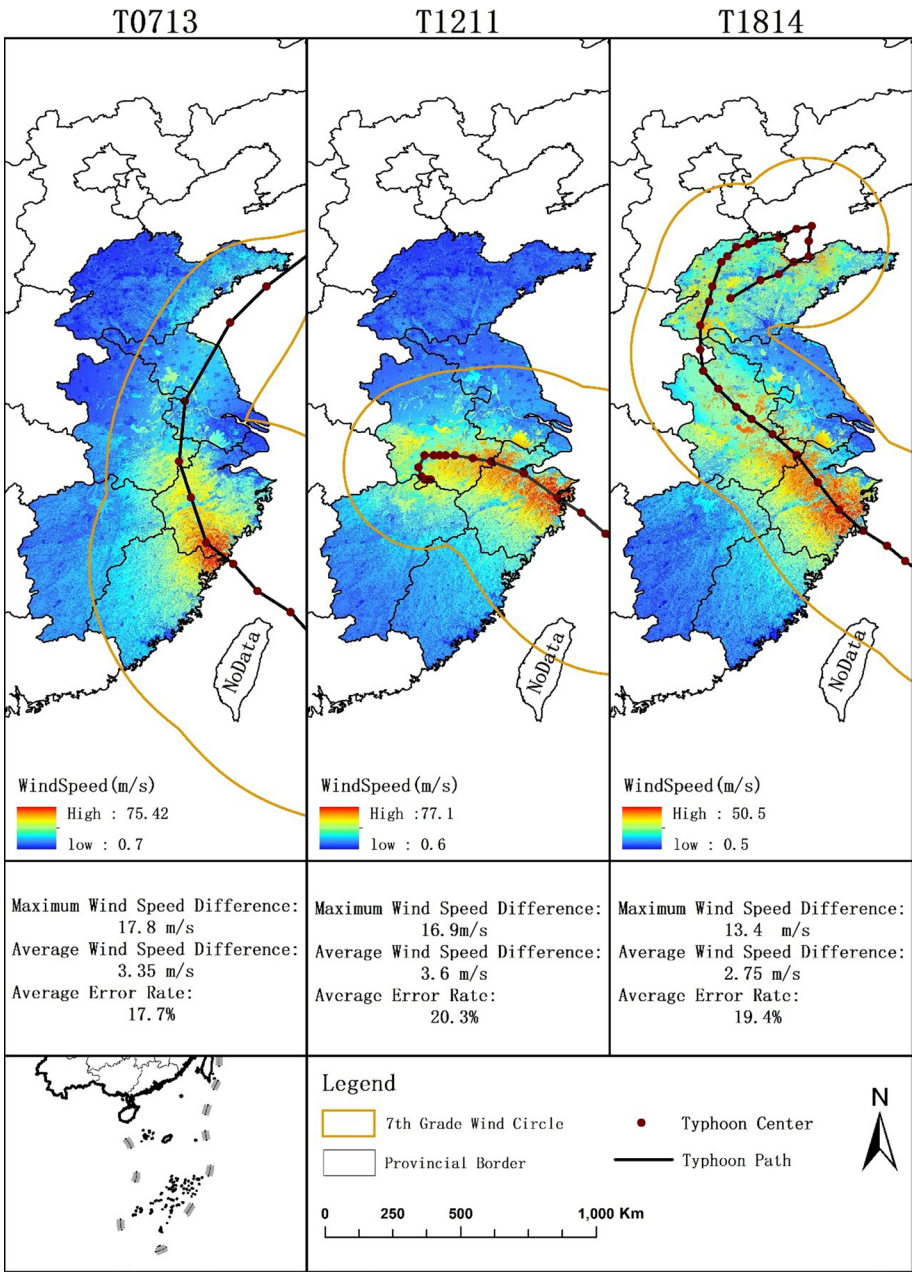

Fig. 3 Simulation results of the typhoon wind fields based on CFD

continuous surface. Based on Fig. 4, the wind field model based on CFD can not only reflects the typhoon process on a large scale but also reflects the spatial variation of the local wind speed distribution in a small-scale area.

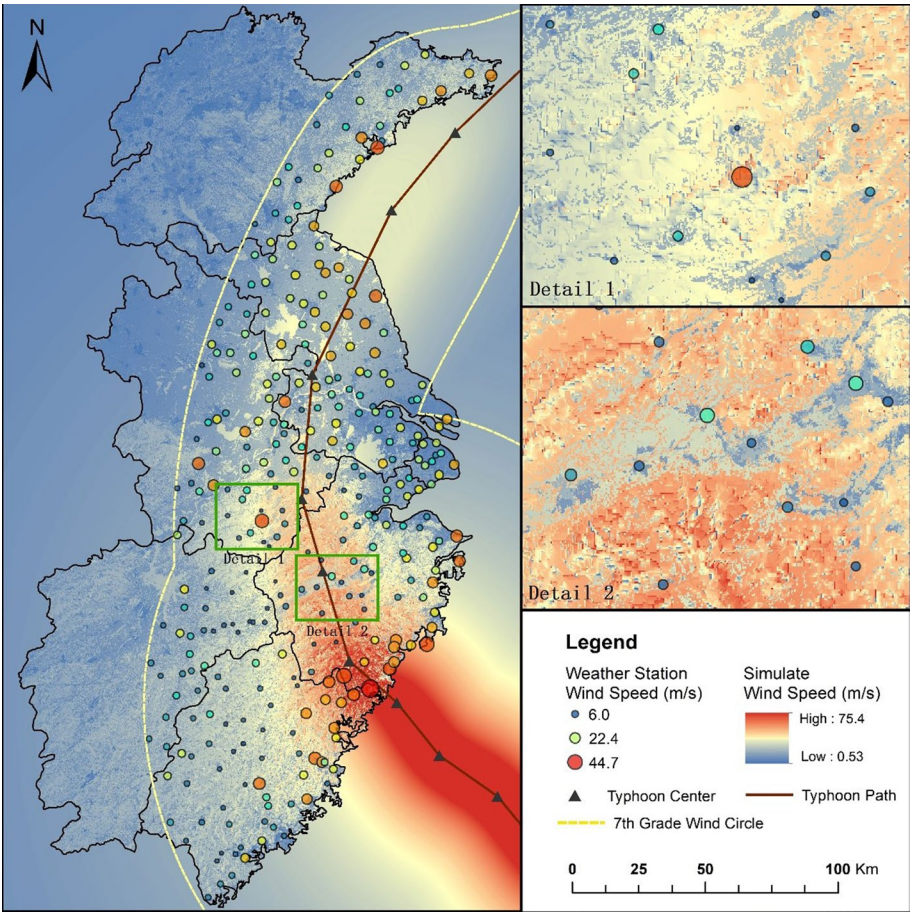

Fig. 4 Spatial comparison of the simulation results of Typhoon No. 0713

We used different typhoon wind field models to simulate the wind speed of Typhoon No. 0713 and selected the same meteorological station within the 7-level wind circle for point-to-point verification for each model. The local simulation effect of the CFD typhoon wind field model was explored by comparing the simulation accuracy of different wind field models horizontally (Table 2).

Compared with the simulation results that ignore the terrain and the commonly used simulation results, the average error rate of the CFD-based typhoon wind field model decreased by 16.89% and 8.8%, respectively. And the absolute difference of the maximum wind speed decreased by 41.5% and 16%, respectively.

To further explore the simulation effect of the wind field model based on CFD, Zhejiang Province with undulating terrain, Jiangsu Province with mainly flat terrain and Shandong Province with balanced terrain were separately selected for the wind speed analysis. The measured wind speed and simulated wind speed at the weather stations are compared in Fig. 5.

Taking topography as the main difference factor for analysis, the average error rate for the 62 meteorological stations in Zhejiang Province is 39%. Compared with other models

Table 2 Simulation results of Typhoon No. 0713 with different typhoon wind field models

Models	Absolute value of maximum wind speed difference (m/s)	Average wind speed difference(m/s)	Average error rate (%)
Typhoon wind field model ignoring the influence of terrain (Holland 2008)	27.97	9.3	34.63
Typhoon wind field models based on building codes (Building Structure Load Code 2012)	21.12	6.1	26.54
Typhoon near surface wind field based on CFD	17.82	3.35	17.74

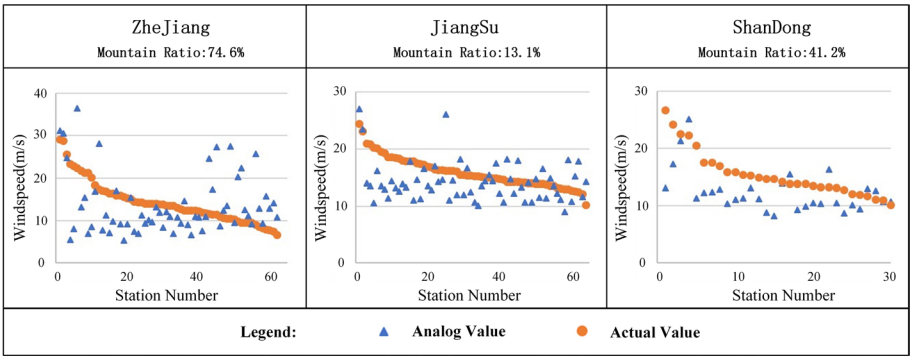

Fig. 5 Regional statistics of the Typhoon No. 0713 simulation results

with error rates of 107.9% and 62.29%, the simulation accuracy is significantly improved, but the overall error rate is relatively high within the range of Typhoon No. 0713. Based on the analysis of the DEM data and land use data, the main errors of Zhejiang's internal wind speed simulation appear in the mountainous areas of western Zhejiang, mainly in mountain basins and canyons, indicating that the existing CFD-based typhoon wind field model is insufficient for the correction of blocked terrain. For Jiangsu Provinces where the terrain is flat, the simulation error reaches 18.1%, respectively, which is better than the simulation results of all affected areas combined. The terrain within the magnitude 7 wind circle in Shandong Province is relatively balanced, and most of the 30 stations included are close to the coast. The overall simulation results of Shandong Province are relatively small, and the simulation error is 23.5%.

For the entire process of Typhoon No. 0713, the intensity of the typhoon successively decreases in Zhejiang, Jiangsu and Shandong. In Zhejiang, where the typhoon intensity is strong, the absolute value of the wind speed is relatively large, and a slight change in the topographical influence factor will worsen the simulation results. With significant changes, the error distribution between the simulation results and the actual value is more scattered than the distributions in the other two provinces. In Jiangsu and Shandong Provinces, where typhoons are weaker, the error distributions are more concentrated.

4 Discussion

This study considers mainly the influence and effects of terrain correction on large-scale typhoon wind field simulations. Therefore, in the process of simulating the wind speed of typical terrain through CFD, only one common roughness parameter suitable for common land-use types is used, and the influence of complex roughness on wind speed is not considered.

Compared with other models, the simulation accuracy of the results of the method in this paper is greatly improved in mountainous areas and other regions with highly complex terrain, but the error in areas with relatively flat terrain remains high. On the one hand, for areas with large terrain undulations the CFD-based terrain correction factor is more accurate than the usual correction methods; on the other hand, the influence of

the terrain on the wind speed in real situations is very complicated, such as the mutual influence between mountains.

Other possible sources of error include the following: Areas dominated by plains may be more susceptible to the effects of roughness of different land-use types. In the gradient layer wind field model, when the typhoon center pressure is high and the typhoon intensity is weak, the simulated wind speed value tends to be low.

Generally, the simulation results of the typhoon wind field model based on CFD terrain correction can accurately reflect the spatial difference and range of typhoon wind hazard factors that are vastly improved compared to the conventional typhoon wind field model, particularly for undulating. The results of this paper can provide technical support or reference information for typhoon disaster risk assessment, loss risk assessment and its application.

5 Conclusion

Using CFD to perform large-scale typhoon wind field simulation and calculation, we discovered problems such as overestimation and underestimation of the wind speed in the terrain correction method based on the building wind load specification. This paper combines the advantages of CFD simulation of a small-scale complex terrain wind speed field with the calculation characteristics of a large-scale terrain correction method in wind load. We also proposed a large-scale complex terrain correction method to simulate the near-surface typhoon wind field. The main conclusions are as follows:

(1) Using CFD to simulate the wind field distribution of small-scale terrain with four different shapes, four different slopes and two initial wind speeds, the wind speed distribution at the peak and foot of the mountain is directly related to the slope of the mountain, and the wind speed distribution on the slope shows similar patterns
(2) CFD simulation results for typical topographic data for statistical analysis show that the windward foot summit point that is characterized by the leeward wind speed corresponding to the foot of the topographical features, yields better indicator fitting results. Compared with the terrain correction method in the building structure load code, the method in this paper can more accurately describe the wind speed distribution and the wind speed changes.
(3) For the typhoon wind field terrain correction based on CFD simulation, a larger-scale wind field can characterize the spatial distribution and intensity differences and more substantially improve the simulated near-surface region of the wind typhoon. Compared with the simulation results of the typhoon wind field that ignores the influence of terrain and load codes, the accuracy improves by 16.89% and 8.8%, respectively.

Supplementary Information The online version contains supplementary material available at https://doi.org/10.1007/s11069-022-05394-9.

Funding This research was funded by the National Key Research and Development Program of China, Grant Numbers 2017YFA0604903 and 2017YFA0604904, which are funded by the Ministry of Science and Technology of the People's Republic of China.

Declarations

Conflict of interest We declare that we have no financial and personal relationships with other people or organizations that can inappropriately influence our work, there is no professional or other personal interest of any nature or kind in any product, service and/or company that could be construed as influencing the position presented in, or the review of, the manuscript entitled.

Consent for publication This paper is original and has not been published elsewhere. The process and results are true presentations and have not been tamper with or forge. The research involved in this paper is not a complete process, and the research has not been divided to publish a larger number of papers. The relevant literature cited is needed for support, and there are no improper self-citations.

References

Alexander D (2000) Confronting catastrophe: new perspectives on natural disasters. Oxford University Press, Oxford

ASTGTM https://lpdaac.usgs.gov/products/astgtmv003/. https://doi.org/10.5067/ASTER/ASTGTM.003

Building structure load code [S]. GB50009-2012. 2012 (**in Chinese**)

Cheng CK, Yuen KK, Lam KM, Lo SM (2005) CFD wind tunnel test: field velocity patterns of wind on a building with a refuge floor. Int J Comput Fluid Dyn 19(7):531

Cheng H, He J, Xu X, Zou X, Wu Y, Liu C, Dong Y, Pan M, Wang Y, Zhang H (2015) Blown sand motion within the sand-control system in the southern section of the Taklimakan Desert Highway. J Arid Land 7(5):599–611

Dong L, Li JZ, Xu YJ, Yang YT, Li XM, Zhang H (2021) Study on the spatial classification of construction land types in Chinese cities: a case study in Zhejiang Province. Land 10(5):523

Grasshopper, https://www.grasshopper3d.com/page/tutorials-1

Griffiths A, Middleton J (2010) Simulation on separated flow over two-dimensional hills. J Wind Eng Ind Aerodyn 98(3):155–160

Holland GJ (1980) An analytic model of the wind and pressure profiles in hurricanes. Mon Weather Rev 108(8):1212–1218

Holland GJ (2008) A revised hurricane pressure: wind model. Mon Weather Rev 136(9):3432–3445

Ishihara T, Hibi K, Oikawa S (1999) A wind tunnel study of turbulent flow over a three-dimensional steep hill. J Wind Eng Ind Aerodyn 83:95–107

Jinping O, Zhongdong D, Liang C (2002) Analysis of typhoon hazard in key cities along the Southeast coast of China. J Nat Disasters 04:9–17 (**in Chinese**)

Ladybug, https://ladybug-tools.gitbook.io/butterflyprimer/

Li Z, Wei Q, Sun Y (2010) Influence of mountain topography on wind vibration response of transmission tower. Power Grid Technol 34(11):214–220. https://doi.org/10.13335/j.1000-3673.pst.2010.11.001 (**In Chinese**)

Li ZL, Xu SY, Xiao ZZ et al (2016) Detailed interpolation distribution of wind speed and terrain correction coefficients along mountain slopes. J Hunan Univ 43(03):23–31. https://doi.org/10.16339/j.cnki.hdxbzkb.2016.03.00 (**In Chinese**)

Lin W, Fang W (2013) Research on the regional characteristics of Holland B coefficient in the northwest pacific typhoon wind field model. Trop Geography 33(02):124–132 (**In Chinese**)

Lou WJ, Liu MM, Li ZH et al (2016) Research on mean wind speed characteristics and speed-up effect in canyon terrain. J Hunan Univ 43(7):8–15 (**In Chinese**)

Lu XQ, Yu H, Ying M, Zhao BK, Zhang S, Lin LM, Bai LN, Wan RJ (2021) Western North Pacific tropical cyclone database created by the China meteorological administration. Adv Atmos Sci 38(4):690–699. https://doi.org/10.1007/s00376-020-0211-7

Maharani YN, Lee S, Lee YK. (2009) Topographic effects on wind speed over various terrains: a case study for Korean Peninsula. In: The Seventh Asia-Pacific conference on wind engineering. Taipei

Ngo TT, Letchford CW (2009) Experimental study of topographic effects on gust wind speed. J Wind Eng Ind Aerodyn 97(9–10):426–438

Qian Li, Zhongdong D (2005) Shapiro typhoon wind field model and its numerical simulation. J Nat Disasters 01:45–52 (**in Chinese**)

Shen GH, Yao D, Lou WJ et al (2016) Investigation of the wind field characteristics on Isolated hill and two adjacent hills using CFD numerical simulation. J Hunan Univ 43(1):37–44 (**In Chinese**)
Shun K, Huirong W (2009) Discussion on the feasibility of applying CFD to the prediction of wind speed distribution in wind farms. J Eng Thermophys 29(12):2400–2042
Uchida T (2018) Computational fluid dynamics approach to predict the actual wind speed over complex terrain. Energies 11(7):1694
Vickery PJ, Dhiraj W (2008) Statistical models of Holland pressure profile parameter and radius to maximum winds of hurricanes from flight-level pressure and H*Wind data. J Appl Meteorol Climatol 47(10):2497–2517
Weihua F, Wei L (2013) Summary of research on typhoon wind field models for disaster risk assessment. Geographical Sci Progress 32(06):852–867 (**in Chinese**)
Ying M, Zhang W, Yu H, Lu X, Feng J, Fan Y, Zhu Y, Chen D (2014) An overview of the China Meteorological Administration tropical cyclone database. J Atmos Oceanic Technol 31:287–301. https://doi.org/10.1175/JTECH-D-12-00119.1

Publisher's Note Springer Nature remains neutral with regard to jurisdictional claims in published maps and institutional affiliations.

Authors and Affiliations

Youtian Yang[1] · Lin Dong[1] · Jiazi Li[1] · Wenli Li[1] · Dan Sheng[1] · Hua Zhang[2,3]

Youtian Yang
201921051167@mail.bnu.edu.cn

Lin Dong
201921051152@mail.bnu.edu.cn

Jiazi Li
202021051160@mail.bnu.edu.cn

Wenli Li
202121051168@mail.bnu.edu.cn

Dan Sheng
202121051172@mail.bnu.edu.cn

[1] Faculty of Geographical Science, Beijing Normal University, Beijing 100875, China

[2] School of National Security and Emergency Management, Beijing Normal University, Beijing 100875, China

[3] China Academy of Education and Social Development, Beijing Normal University, Beijing 100875, China